



This is a repository copy of *Downstream MET-IRSL single-grain distributions in the Mojave River, southern California: Testing assumptions of a virtual velocity model.*

White Rose Research Online URL for this paper:
<http://eprints.whiterose.ac.uk/108892/>

Version: Accepted Version

Article:

McGuire, C and Rhodes, EJ (2015) Downstream MET-IRSL single-grain distributions in the Mojave River, southern California: Testing assumptions of a virtual velocity model. *Quaternary Geochronology*, 30. pp. 239-244. ISSN 1871-1014

<https://doi.org/10.1016/j.quageo.2015.02.004>

Article available under the terms of the CC-BY-NC-ND licence
(<https://creativecommons.org/licenses/by-nc-nd/4.0/>)

Reuse

Unless indicated otherwise, fulltext items are protected by copyright with all rights reserved. The copyright exception in section 29 of the Copyright, Designs and Patents Act 1988 allows the making of a single copy solely for the purpose of non-commercial research or private study within the limits of fair dealing. The publisher or other rights-holder may allow further reproduction and re-use of this version - refer to the White Rose Research Online record for this item. Where records identify the publisher as the copyright holder, users can verify any specific terms of use on the publisher's website.

Takedown

If you consider content in White Rose Research Online to be in breach of UK law, please notify us by emailing eprints@whiterose.ac.uk including the URL of the record and the reason for the withdrawal request.



eprints@whiterose.ac.uk
<https://eprints.whiterose.ac.uk/>

1 Downstream MET-IRSL single-grain distributions in the Mojave River, 2 southern California: Testing assumptions of a virtual velocity model

3
4 Christopher McGuire¹ & Edward J. Rhodes^{1,2}

5
6 1 Earth, Planetary and Space Sciences, UCLA, Los Angeles, USA

7 2 Dept. of Geography, University of Sheffield, Sheffield, S10 2TN, UK

8
9 Author's accepted version of a paper published in Quaternary Geochronology 30, 239-244 (2015)

10 <http://dx.doi.org/10.1016/j.quageo.2015.02.004>

11 12 13 Abstract

14 We use samples from a prior study (McGuire and Rhodes, 2015) to investigate the bleaching trend of
15 Mojave River sand in more detail. We present new single grain data which provides insight into how
16 previously presented multiple-grain luminescence signals decrease downriver. The single grain dose
17 distributions allow for a test of the assumption that multiple-grain equivalent dose (D_e) is representative
18 of fluvial transport down the Mojave River. For samples at the Forks, Victorville and Barstow, with
19 laboratory luminescence sample codes J0262, J0267 and J0265, respectively, inspection of the kernel
20 density estimate (KDE)-generated probability density function supports the assumption, though it does
21 not prove it directly. Implementing a Kolmogorov–Smirnov (K–S) test shows that the downriver samples
22 are statistically different from each other, suggesting bleaching as the primary mechanism for changes in
23 dose distribution downriver. Single-grain dose distributions show that the D_e of the Afton Canyon
24 sample (J0260) is not representative of grain travel from source to sink, but instead likely a result of local
25 mixing of sediment populations. This result is confirmed by visual inspection of the KDE, and
26 quantitatively using the K–S test. As has been noted by several authors, the single-grain dose
27 distribution in active channels of rivers may represent a worst case in terms of poor bleaching, due to
28 mixing of older-age populations (Cunningham et al., 2014; Jain et al., 2004). This observation holds for
29 our data set and presents an opportunity to test and develop luminescence techniques to determine
30 provenance. In particular, future sampling in the vicinity of the Afton Canyon site has the potential to
31 identify the entry point of a poorly-bleached population.

32 33 Keywords

34 Mojave River

35 Luminescence

36 Geomorphology

37 MET-pIRIR

38 39 Introduction:

40 Fluvial sediments of Holocene and Pleistocene age are now routinely dated using feldspar grains
41 due in part to the development of the post-infrared stimulated luminescence (pIRIR) protocol (Rhodes,
42 in press; Buylaert et al., 2009; Li & Li, 2011). This technique was developed to obtain an IRSL signal from
43 feldspar that does not fade, or fades very little over the time scale of interest (Li & Li, 2011). A possible
44 drawback to the technique is that sequential, higher temperature measurements of the pIRIR protocol
45 bleach more slowly in sunlight and underwater than standard IRSL signals (Kars et al., 2014). In a
46 previous study, we took advantage of the tendency of pIRIR signals to be poorly bleached in order to

47 obtain information about the rate of travel of fine sand in the Mojave River (McGuire & Rhodes, 2015;
48 Reimann et al., 2015). A fundamental assumption of that study was that fluvial transport is the
49 dominant cause of differences in multiple-grain (MG) D_e along the river. Several workers have shown
50 that inferences about degree of partial bleaching from MG aliquots are subject to grain sensitivity and
51 aliquot size, both of which are difficult to control for using only MG data (Cunningham et al., in press;
52 Arnold & Roberts 2009). In the present study, we make single-grain (SG) measurements of a subset of
53 the samples presented previously (McGuire & Rhodes, 2015). The implementation of SG measurement
54 techniques has allowed for analysis of poorly bleached fluvial sediments using robust statistical models
55 (Roberts et al., 2000; Bailey & Arnold, 2006; Arnold et al., 2007). In this study, we examine SG equivalent
56 dose (D_e) populations graphically using kernel density estimate (KDE)-generated probability distributions
57 and quantitatively using the Kolmogorov-Smirnov (KS) test.

58

59 Samples and Methods:

60 Samples were collected from shallow pits in channel and point bars in the modern Mojave River.
61 The sample locations and laboratory codes are shown in Figure 1. The depth of the samples ranged from
62 30 – 80 cm; the range was due to our field protocol that samples be collected only where bedding
63 structures are present, in order to reduce the effects of recent bioturbation. The 175-200 μm grain size
64 fraction was chosen for measurement, with the exception of sample J0266, for which there was
65 insufficient material in the desired grain size range, and the 200 – 220 μm range was selected.
66 Mineralogical separation was done using lithium metatungstate liquid, diluted to a density of 2.58 gcm^{-3} ,
67 as our lab had not yet implemented Super-K (2.565 gcm^{-3}) density separation (Rhodes, in press). The
68 possible inclusion of sodic-rich feldspars after density separation may affect the changes in dose
69 distributions downriver (see Discussion). Samples were treated with HCl to remove carbonates. The
70 location of samples along with their laboratory codes (J0260 to J0267) are the same as previously
71 reported and are shown in Figure 1. Single-aliquot D_e of these samples was measured and described
72 previously (McGuire and Rhodes, 2015). In this study, we present results from single-grain (SG) MET-
73 pIRIR measurements and thermoluminescence measurements of a subset of the samples. We
74 implement a MET-pIRIR measurement protocol, adapted for single-grains (Fu & Li, 2013; Reimann et al.,
75 2012). Single-grain discs from a subset of Mojave river samples were measured at temperature
76 increments of 50, 95, 140, 185 and 230 $^{\circ}\text{C}$; the full measurement protocol is shown in the table S1.
77 Additionally, we measured thermoluminescence (TL) of small aliquots and the measurement protocol is
78 shown in Table S2. It is important to note that fading corrections were not made for the SG MET-pIRIR
79 measurements nor the TL measurements; therefore, the equivalent doses of individual grains cannot be
80 interpreted to indicate an age.

81

82 Results:

83 The shape of TL D_e as a function of distance downriver differs in general from the MG MET-pIRIR
84 trends. The concave-down shape of the TL data (as opposed to a concave-up stretched exponential) is
85 likely a result of the reduced bleachability of feldspar TL in the water column when compared to optical
86 luminescence bleaching (Rendell et al., 1994; Berger, 1990). The TL measurements, in conjunction with
87 the MG MET-pIRIR trends, provide evidence for a decreasing degree of bleaching in the water column

88 with distance downriver. This inference is supported by hydrologic data, which shows that transmission
89 and evaporation loss of surface water is significant downriver, even for the largest floods (Figure 3).

90 Single-grain data were processed using Riso's software Analyst. Rejection criteria applied to
91 grains were >100% error in dose, >50% recycling ratio limit and the inability to fit the dose response
92 curve with an exponential or exponential plus linear function in Analyst. Single-grain dose distributions
93 for each temperature and sample are represented with a kernel density estimate (Figure 4). General
94 trends from graphical inspection can be grouped into two categories: intra-sample and inter-sample.
95 The intra-sample trends show that the grain population is progressively more poorly bleached at higher
96 pIRIR measurement temperature. This observation is based on the widening of highest relative
97 probability peak with increasing temperature. Additionally, the number of grains returning signal
98 decreases with increasing measurement temperature. This may reflect a mixed mineralogy as density
99 separation was done at 2.58 g cm^{-3} (instead of 2.565 g cm^{-3}), which can cause plagioclase feldspar to be
100 included in the SG population (Rhodes, in press). The decreasing number of grains returning signal may
101 also indicate a reduced probability of recombination with increasing temperature (Poolton et al., 2001),
102 resulting in low signal to noise ratio for the lowest dose fraction of grains. While this observation casts
103 some doubt on the extent of extrapolations that can be made from SG MET-pIRIR dose distributions,
104 inter-sample trends show that bleaching has a first order effect on the shape of the SG MET-pIRIR D_e
105 distributions. The SG MET-pIRIR KDE's show increased bleaching of grains at Barstow relative to the
106 Forks, for each temperature IRSL measurement. The IR_{230} KDE for the Forks shows equal relative
107 probability at a range of D_e (1.87 to 135 Gy), but the IR_{230} KDE for Barstow a relative probability peak (at
108 ~ 18 Gy) emerges (Figure 4b), suggesting that bleaching has occurred.

109 Statistical Tests:

110 We use the two-sample Kolmogorov-Smirnov (KS) test to determine whether dose distributions
111 are statistically different from each other. The test uses empirical cumulative distribution functions
112 (ecdf's) for two samples and calculates the "distance" in cumulative probability between samples (see
113 Conover, 1999). The test determines between the null hypothesis (H_0) that the distributions are the
114 same and the alternative hypothesis (H_1) that the distributions are different, to some confidence level α
115 (in this case, set to 0.05). The KS test for the Forks and Barstow SG distributions rejects H_0 , which leads
116 us to conclude, as expected, that the deposits are different (Figure 5). This result provides statistical
117 justification for exploring the reason for the difference. The KS test for Barstow and Afton Canyon fails
118 to reject H_0 , which suggests (though does not prove) that the increased MG D_e at Afton Canyon relative
119 to Barstow is due to the contribution of a few locally-sourced, poorly-bleached grains.

120 Roberts et al., (2000) found that it is possible to distinguish dose populations as long as there is
121 a small number of mixture components. Since the SG data for Afton Canyon appear to be a mixture of a
122 Barstow-provenance population and an unknown-provenance population, further sampling of the
123 surrounding sedimentary facies and tributaries may reveal both the source and the proportion of mixing
124 of the older population. The Afton Canyon sample was collected at a location where the Mojave River
125 has incised through Quaternary-Tertiary fanglomerates (Reheis & Redwine, 2008). Sediment delivered
126 through tributaries could be the source of the higher equivalent dose population, as saturated grains
127 from the fanglomerates are partially bleached over the short transport distance to the modern Mojave
128 River channel. Alternative explanations include entrainment fine sand fractions from Lake Manix, a
129 Pleistocene pluvial lake that was the ancestral terminus of the Mojave River before Afton Canyon was

130 incised (Reheis et al., 2012; Enzel & Wells, 1997). Further sampling in the region has the potential to
131 resolve the proportion of mixing of the Mojave River population and the older, poorly-bleached
132 population.

133 Discussion:

134 The trends observed in SG MET-pIRIR equivalent dose distributions for the Forks and Barstow
135 are consistent with increased bleaching of grains down the Mojave River. A 3-component finite mixture
136 model using MATLAB function `gmdistribution.fit` function for each IR-50 °C distribution showed
137 that the lowest mixture component shifts from 1.73 Gy at the Forks to 0.27 Gy at Barstow. The shift to
138 lower D_e is accompanied by a reduction in the tail of the relative probability peak. This observation may
139 be due to better bleaching of grains. However, it could also be due to the weathering of plagioclase
140 down the river. Inclusions of plagioclase grains in the SG population may increase scatter, due to
141 different luminescence characteristics (Lamothe & Auclair, 1997; Prescott et al., 1994). Plagioclase
142 signals are generally less bright than K-feldspar signals, especially at higher temperatures, so it is
143 possible that plagioclase distributions are excluded from higher temperature dose distributions. An
144 additional factor complicating the interpretation of number of KDE plots (Figure 4) is that the number of
145 accepted grains decreases with increasing measurement temperature. The IRSL signal's dependence on
146 temperature is likely representative of the presence of plagioclase in the sample, as described above,
147 but may also represent a reduction in recombination probability, resulting in rejection of more grains at
148 higher temperature due to lower signal to noise ratio. Future sampling in the region, and density
149 separation using Super-K (2.565 g cm^{-3}) should help resolve this issue (Rhodes, in press). The KS-test can
150 be dependent on the number of observations and since there are more observations at Afton Canyon (n
151 = 235) than at Barstow (n = 173) for IR₅₀, it is possible that the test is affected, however, we note that
152 more observations tend to drive the KS-test toward rejection (Joel Saylor, pers. comm.), which is the
153 opposite result reported here. Still, we acknowledge that the KS-test is limited in its ability to determine
154 whether two samples are drawn from different populations.

155 Attributing the bleaching of grains to fluvial transport, as opposed to aeolian transport or
156 selective weathering is a difficult task. The episodic nature of water flow on the Mojave River could
157 allow for the majority of bleaching to occur on the surface after deposition (Gray & Mahan, 2015),
158 resulting in similar D_e distributions for movement of grains by wind or water. The MG MET-pIRIR trends
159 in both dose and error (Figure 2) are consistent with a theoretical model for episodic surface bleaching
160 (Gray & Mahan, 2015). In this model, standard deviation decreases downriver along with D_e , as the
161 grains become better mixed and bleached. In this model, the introduction of a new population causes
162 the D_e and standard deviation to increase (Harrison Gray, pers. comm.), which is the case for our data
163 set, specifically at Afton Canyon. We attribute the higher MG D_e and standard error at Afton Canyon to
164 the few higher dose grains in the SG dose distribution, but note that aliquot size of the MG discs could
165 affect the apparent trend (Cunningham et al., in press). These observations support the argument that
166 at least a portion of the bleaching is occurring on the surface, after grains are deposited.

167 In a more complicated scenario, some linear combination of surface bleaching after deposition
168 and underwater bleaching during floods could occur. One indication that surface bleaching alone cannot
169 explain SG downriver trends is that a bimodal distribution of equivalent doses does not occur, as an
170 episodic surface bleaching model predicts (Gray & Mahan, 2015) Another line of evidence is that a
171 stepwise MG pIRIR model (McGuire & Rhodes, 2015) based on full-sunlight empirical bleaching curves

172 consistently under-predicts IR₅₀, IR₉₅ and IR₁₄₀ values down the river in all model runs. These lower
173 temperature pIRIR signals have reached a constant value between sample J0266 and Barstow (J0265),
174 possibly related to the pIRIR residual value, which is a function of both deposition environment and
175 pIRIR measurement temperature (Figures 1, 2). Controlled bleaching experiments to simulate the effects
176 of wavelength filtering in the water column have shown that residual IRSL signal increases linearly with
177 pIRIR measurement temperature (Kars et al., 2014). It is possible that the higher than modelled (see
178 McGuire & Rhodes, 2015) MG D_e of IR₅₀, IR₉₅ and IR₁₄₀ represents the effects of water-lain bleaching. A
179 secondary line of evidence presented in this paper is that the downriver change in TL D_e does not follow
180 the same stretched exponential shape of the MET-pIRIR measurements (Figure 2). Since the TL signal is
181 much less bleachable underwater than the optical signal (Rendell et al., 1994), the lack of significant
182 reduction in TL signals suggest that some of the bleaching is occurring underwater.

183 In order to test whether the single-grain distributions observed could result primarily from
184 fluvial processes, we developed further the model presented in McGuire & Rhodes (2015). The model
185 supposes that sediment is mobilized when river discharge is above a certain threshold (e.g. bankfull
186 discharge). Discharge for the Mojave River is modelled using the Helendale USGS station (10260950)
187 historical data fitted to a generalized Pareto distribution for all values greater than zero using maximum
188 likelihood estimation. Values that are zero discharge are approximated from the data and resampled in
189 MATLAB using an if-statement. A summary of methods for treating discharge data with excess zeros can
190 be found in Weglarczyk et al. (2005). The model produces a random number from the Helendale
191 generalized Pareto parameterization and applies an arbitrary threshold for bleaching: in the simulation
192 presented in Figure 6, 10 m³s⁻¹ was used. If the number representing discharge is above the threshold,
193 we assume the sand will bleach according to the experimentally determined bleach parameters of the
194 general order kinetics equation (see McGuire & Rhodes, 2015). If discharge is below the threshold or
195 zero, the sand will remain buried and the dose response curve, determined experimentally for the MG
196 discs (see McGuire & Rhodes, 2015) is used to represent signal growth during burial (Murray and Wintle,
197 2003). This process was repeated for 2000 iterations, with time-steps of one month. The process was
198 then repeated 200 times to simulate various grain histories that are possible after successive iterations.
199 The resulting synthetic distributions are shown in Figure 6. These results suggest that it is possible to
200 produce the trend towards better bleached samples downriver simply from random fluctuations in the
201 frequency of bleaching. Additionally, the data can be re-produced closely, if the best-fitting iteration is
202 selected.

203 Another finding of this paper is that contribution of a mixing population can have a first order
204 effect on downriver trends of pIRIR signals, as is the case at Afton Canyon. We propose that the SG dose
205 distribution at Afton Canyon results from a small contribution of locally-sourced grains mixed with a SG
206 dose distribution similar to the Barstow sample (J0265). The implications of this hypothesis are that (1)
207 tributary and/or terrace erosion exert a first order control on MG dose, and that (2) if the input
208 population of locally sourced sand has a significantly different D_e from the main channel sand, its
209 signature could be removed. The presence of this higher dose population may allow for future sampling
210 along the river to pinpoint the location of the routing of these poorly bleached grains. This has
211 important implications for provenance studies using luminescence equivalent dose distributions.

212 Conclusion:

213 Single-grain MET-pIRIR distributions are used to show that D_e populations at the Forks and
214 Barstow differ in a statistically significant way, consistent with a trend towards better bleaching
215 downriver. This result supports the possibility that changes in D_e down a river could be combined with
216 theoretical models to gather information about sediment transport. The single-grain results at Afton
217 Canyon show that using multiple-grain aliquots could be misleading, as the influence of mixed, older
218 populations could go undetected. In this case, the model of Gray and Mahan (2015) correctly predicts
219 that the Afton Canyon D_e is a result of mixing and not burial time. The first-order influence of mixing
220 populations on a modern sample provide support for the use of luminescence in provenance studies
221 (Zular et al., 2013). Jain et al., (2004) argue that modern fluvial sand D_e distributions from the Loire River
222 represent a poorest-bleaching case. Stokes et al. (2001) and others suggest that bank erosion and
223 tributaries may contribute older grains to the modern channel (Rittenour, 2008; Stokes, 1999). Our data
224 supports these assertions, and we propose further that the modern river channel can be thought of as a
225 gravity well for sediment in the immediate surroundings, routed via the drainage network. Using this
226 general framework, the degree of partial bleaching would be dependent upon local gradient and the
227 dose distribution of up-gradient deposits. We do not propose to test this explanation with the current
228 data set, but rather suggest that interpretations about dose distributions of modern fluvial samples are
229 subject to provenance and the ability of the drainage system to deliver locally sourced sediments.

230 Acknowledgements:

231 We would like to thank Michel Lamothe and Magali Barre for organizing and hosting the LED 2014
232 conference in Montreal. We also thank one anonymous reviewer whose comments and suggestions
233 improved the quality of this manuscript. We acknowledge funding that contributed to the ideas
234 presented in this paper, from NSF EAR-1321912.

235 Figure 1: Map of the Mojave Desert region, showing the drainage basin of the Mojave River and the
236 sample locations (red triangles) with sample laboratory codes. Single-grain and thermoluminescence
237 results for a subset of these samples (J0262, J0266, J0265 and J0260) are reported in this paper (for the
238 entire set of MG MET-pIRIR results, see McGuire & Rhodes, 2015). Map after McGuire & Rhodes (2015).
239 Digital elevation model created using the National Elevation Dataset (Gesch, 2007; Gesch et al., 2002).

240

241 Figure 2: Multiple-grain, single-aliquot equivalent dose is plotted against distance downriver (after
242 McGuire & Rhodes, 2015). Absolute standard error is plotted below for the samples. MET-pIRIR D_e
243 decreases in a stretched exponential shape, then increases for all temperatures at the furthest point
244 downriver (Afton Canyon, J0260). Only three sample were measured with TL, due to lack of material; the
245 trend in TL D_e departs from an exponential shape, indicating that some of the bleaching over this portion
246 of river has occurred underwater.

247

248 Figure 3: Monthly integrated discharge for the Mojave River from 1950 to 1997 is plotted with two
249 models for transmission loss of water down the river. These models connect data points from two
250 individual historic floods. The February, 1993 flood is one of the largest on record, and the discharge still
251 decays down the river. The February 1973 flood is smaller and displays the more frequent discharge

252 shape, in which station 10263000 (Afton Canyon) receives almost no discharge ($\sim 2 \text{ m}^3 \text{ s}^{-1}$). Data from
253 USGS National Water Information System: <http://waterdata.usgs.gov/ca/nwis/uv?site_no=10262500>

254

255 Figure 4: Kernel density estimates (KDE) of the single-grain MET-pIRIR results are plotted by equivalent
256 dose versus relative probability. The number of grains returning signal corresponding with measurement
257 temperature is shown in the legend. Note the scaling of both axes changes. (a) The KDE for the Forks
258 shows several higher-dose populations that are not present at Barstow. The IR₂₃₀ SG results show equal
259 relative probability of a series of D_e, indicating that little to no bleaching of this signal has occurred at
260 this location. A total of 200 grains were analyzed. (b) The KDE for Barstow shows that significant
261 populations are not present in comparison to the Forks. Additionally the IR₂₃₀ KDE shows some evidence of
262 bleaching. A total of 400 grains were analyzed. (c) The Afton Canyon KDE shows a similar, well-bleached
263 peak (note scaling change on rel. prob. axis) to Barstow along with inclusion of several older grains. The
264 IR₂₃₀ KDE also shows evidence of bleaching. A total of 600 grains were analyzed.

265 Figure 5: Empirical cumulative distribution function (ecdf) for IR₅₀ single grains at the Forks, Barstow and
266 Afton Canyon. The ecdf is the basis for the KS test, and, as can be seen from the deviation of the dashed
267 curve from the other curves, a greater proportion of the Forks D_e population differs from Barstow than
268 does the Afton Canyon D_e population.

269

270 Figure 6: Ecdf for IR₅₀ single grains from the Forks and Barstow are shown (open circles) with ecdf for
271 synthetic IR₅₀ single grain distributions in a simple bootstrapped fluvial model (see text for description).
272 One iteration is equivalent to one month of time passed on the Mojave River. The synthetic distributions
273 show that single-grain populations should become better bleached downriver, following the trend
274 shown in the data from the Forks and Barstow.

275

276

277 References:

278 Arnold, L.J., Roberts, R.G., 2009. Stochastic modelling of multi-grain equivalent dose (D_e) distributions:
279 Implications for OSL dating of sediment mixtures. *Quaternary Geochronology*, 4. 204 – 230.

280

281 Arnold, L.J., Bailey, R.M., Tucker, G.E., 2007. Statistical treatment of fluvial dose distributions from
282 southern Colorado arroyo deposits. *Quaternary Geochronology*, 2. 162 – 167.

283

284 Bailey, R.M. & Arnold, L.J., 2006. Statistical modelling of single grain quartz D_e distributions and an
285 assessment of procedures for estimating burial dose. *Quaternary Science Reviews*, 25. 2475 – 2502.

286

287 Berger, G. W., 1990. Effectiveness of natural zeroing of the thermoluminescence in sediments. *Journal of*
288 *Geophysical Research*, 95: 12375 – 12397.

289

290 Buylaert, J. P., Murray, A. S., Thomsen, K. J., and Jain, M., 2009. Testing the potential of an elevated
291 temperature IRSL signal from K-feldspar. *Radiation Measurements*, 44: 560-565.

292 Conover, W.J., 1999. *Practical Nonparametric Statistics*. Wiley, New York.

293 Cunningham, A.C., Wallinga, J., Hobo, N., Versendaal, A.J., Makaske, B., Middelkoop, H., 2014. Does
294 deposition depth control the OSL bleaching of fluvial sediment? *Earth Surface Dynamics*, 2. 575 – 603.

295

296 Enzel, Y. and Wells, S. G., 1997. Extracting Holocene paleohydrology and paleoclimatology information
297 from modern extreme flood events: an example from southern California. *Geomorphology*, 19: 203-226.

298

299 Fu, X., Li, S., 2013. A modified multi-elevated temperature post IR-IRSL protocol for dating Holocene
300 sediments using K-feldspar. *Quaternary Geochronology*, 17: 44-54.

301

302 Gesch, D.B., 2007, *The National Elevation Dataset*, in Maune, D., ed., *Digital Elevation Model*
303 *Technologies and Applications: The DEM Users Manual*, 2nd Edition: Bethesda, Maryland, American
304 Society for Photogrammetry and Remote Sensing, pp 99-118.

305

306 Gesch, D., Oimoen, M., Greenlee, S., Nelson, C., Steuck, M., and Tyler, D., 2002, *The National Elevation*
307 *Dataset: Photogrammetric Engineering and Remote Sensing*, 68: 5-11.

308

309 Gray, H. J., & Mahan, S. A., 2015. Variables and potential models for the bleaching of luminescence
310 signals in fluvial environments. *Quaternary International*.

311

312 Jain, M., Murray, A.S., Botter-Jensen, L., 2004. Optically stimulated luminescence dating: how significant
313 is incomplete light exposure in fluvial environments? *Quaternaire*, 15. 143 – 157.

314

315 Kars, R. H., Reimann, T., Ankjaergaard, C., Wallinga, J., 2014. Bleaching of the post-IR IRSL signal: new
316 insights for feldspar luminescence dating. *Boreas*, 43. 780 – 791.

317

318 Lamothe & Auclair, M., 1997. Assessing the datability of young sediments by IRSL using an intrinsic
319 laboratory protocol. *Radiation Measurements*, 27. 107-117.

320

321 Li, B., Li, S., 2011. Luminescence dating of K-feldspar from sediments: A protocol without anomalous
322 fading correction. *Quaternary Geochronology*, 6: 469-479.

323

324 McGuire, CP., Rhodes, E.J., accepted. Determining fluvial sediment virtual velocity of the Mojave River
325 using K-feldspar: initial assessment. *Quaternary International*, September, 2015.

326

327 Murray, A. S., Wintle, A. G., 2003. The single aliquot regenerative dose protocol: potential for
328 improvements in reliability. *Radiation Measurements*, 37: 337-381.

329

330 Poolton, N.J., Ozanyan, K.B., Wallinga, J., Murray, A.S., Botter-Jensen, L., 2002. Electrons in feldspar II: a
331 consideration of the influence of conduction band-tail states on luminescence processes. *Physics and
332 Chemistry of Minerals*, 29. 217 – 225.

333

334 Prescott, J.R., Fox, P.J., Robertson, G.B., Hutton, J.T., 1994. Three-dimensional spectral studies of the
335 bleaching of the thermoluminescence of feldspars. *Radiation Measurements*, 23. 367 – 375.

336

337 Reheis, M. C., Redwine, J. L., 2008. Lake Manix shorelines and Afton Canyon terraces: Implications for
338 incision of Afton Canyon. Reheis, M.C., Hershler, R., and Miller, D.M., eds., in *Late Cenozoic Drainage
339 History of the Southwestern Great Basin and Lower Colorado River Region: Geologic and Biotic
340 Perspectives: Geologic Society of America, Special Paper 349*, pp 227 – 259.

341 Reheis, M. C., Bright, J., Lund, S. P., Miller, D.M., Skipp, G., Fleck, R. J., 2012. A half-million-year record of
342 paleoclimate from the Lake Manix Core, Mojave Desert, California. *Palaeogeography, Palaeoclimatology,
343 Palaeoecology*, 365, 11 - 37.

344

345 Rittenour, T., 2008. Luminescence dating of fluvial deposits: applications to geomorphic, paleoseismic
346 and archeological research. *Special Issue, Boreas*, 37, 613-635.

347

348 Reimann, T., Thomsen, K.J., Jain, M., Murray, A.S., Frechen, M., 2012. Single-grain dating of young
349 sediments using the pIRIR signal from feldspar. *Quaternary Geochronology*, 11. 28 – 41.

350

351 Reimann, T., Notenboom, P.D., De Schipper, A.M., Wallinga, J., 2015. Testing for sufficient signal
352 resetting during sediment transport using a polymineral multiple-signal luminescence approach.
353 *Quaternary Geochronology*, 25. 26 -36.

354

355 Rendell, H.M., Webster, S.E., Sheffer, N.L., 1994. Underwater bleaching of signals from sediment grains:
356 new experimental data. *Quaternary Science Reviews*, 13. 433 – 435.

357

358 Rhodes, E.J. Dating sediments using potassium feldspar single-grain IRSL: initial methodological
359 considerations. *Quaternary International*, submitted, October 2014.

360

361 Roberts, R.G., Galbraith, R.F., Yoshida, H., Laslett, G.M., Olley, J.M., 2000. Distinguishing dose
362 populations in sediment mixtures: a test of single-grain optical dating procedures sing mixtures of
363 laboratory-dosed quartz. *Radiation Measurements*, 32. 459 – 465.

364

365 Stokes, S., Bray, H.E., Blum, M.D., 2001. Optical resetting in large drainage basins: tests of zeroing
366 assumptions using single-aliquot procedures. *Quaternary Science Reviews*, 20: 879-885.

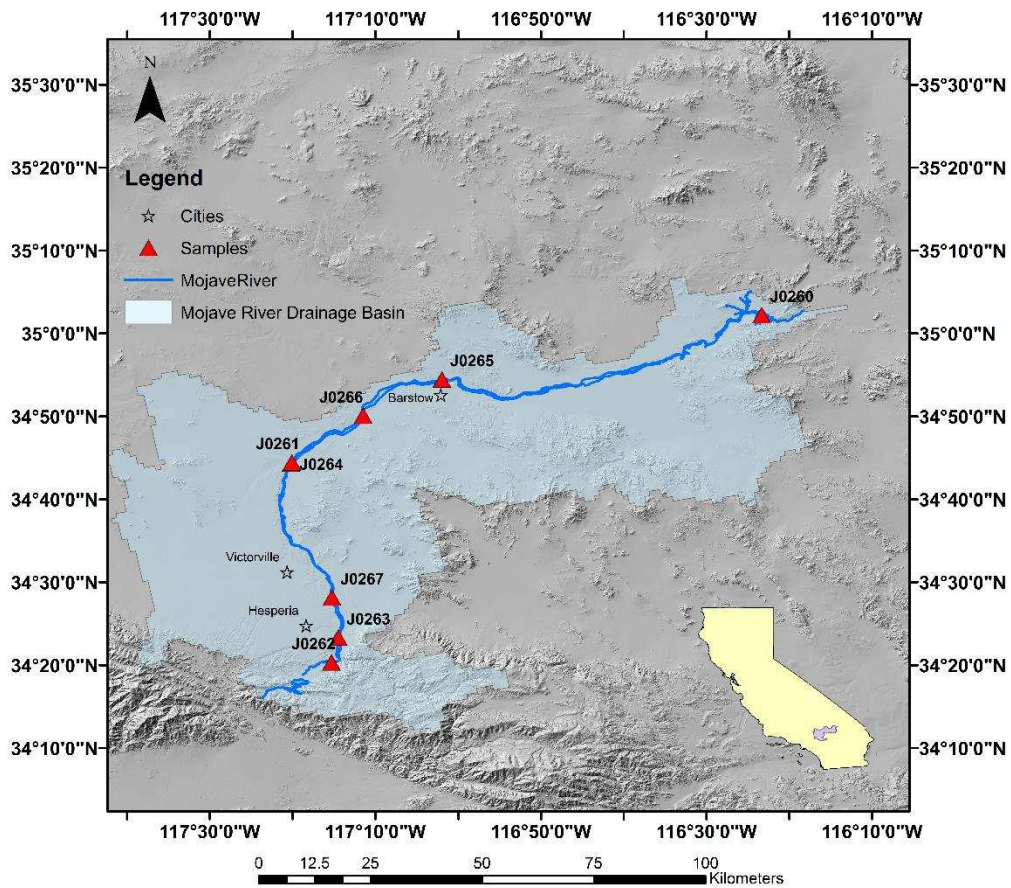
367

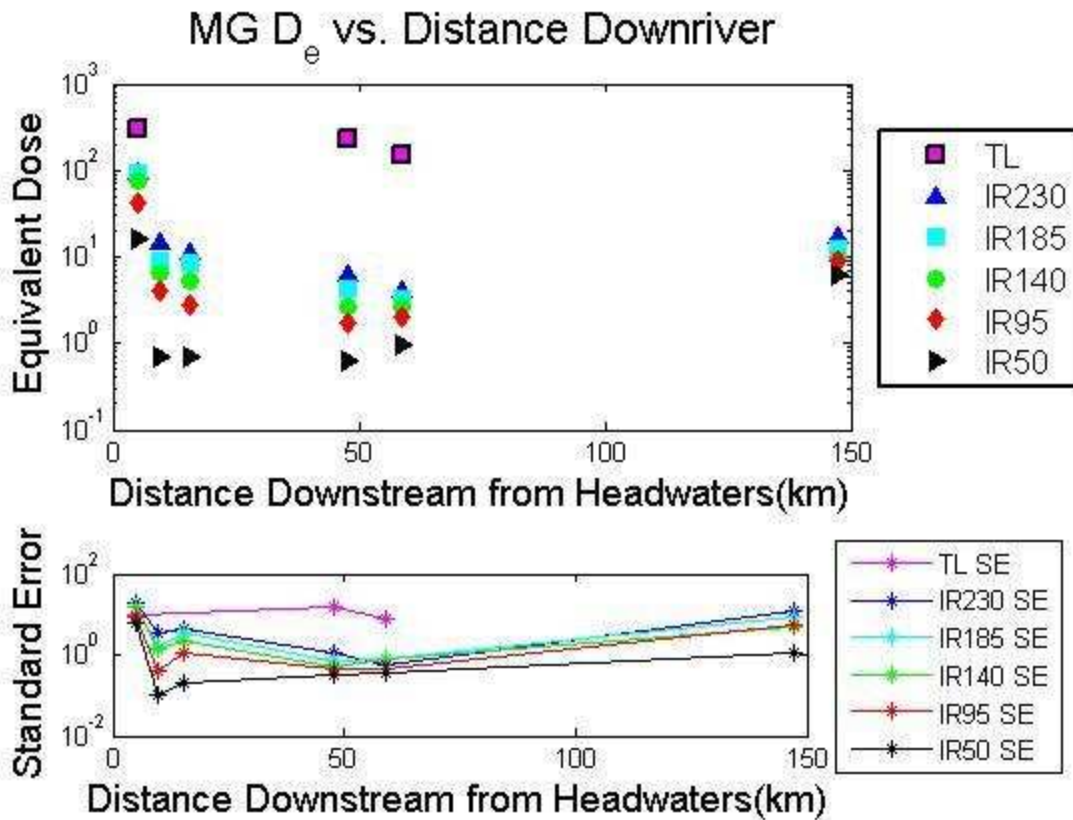
368 Stokes, S., 1999. Luminescence dating applications in geomorphological research. *Geomorphology*, 29:
369 153-171.

370 USGS National Water Information System, http://waterdata.usgs.gov/ca/nwis/uv?site_no=10262500
371 (accessed July 3, 2014).

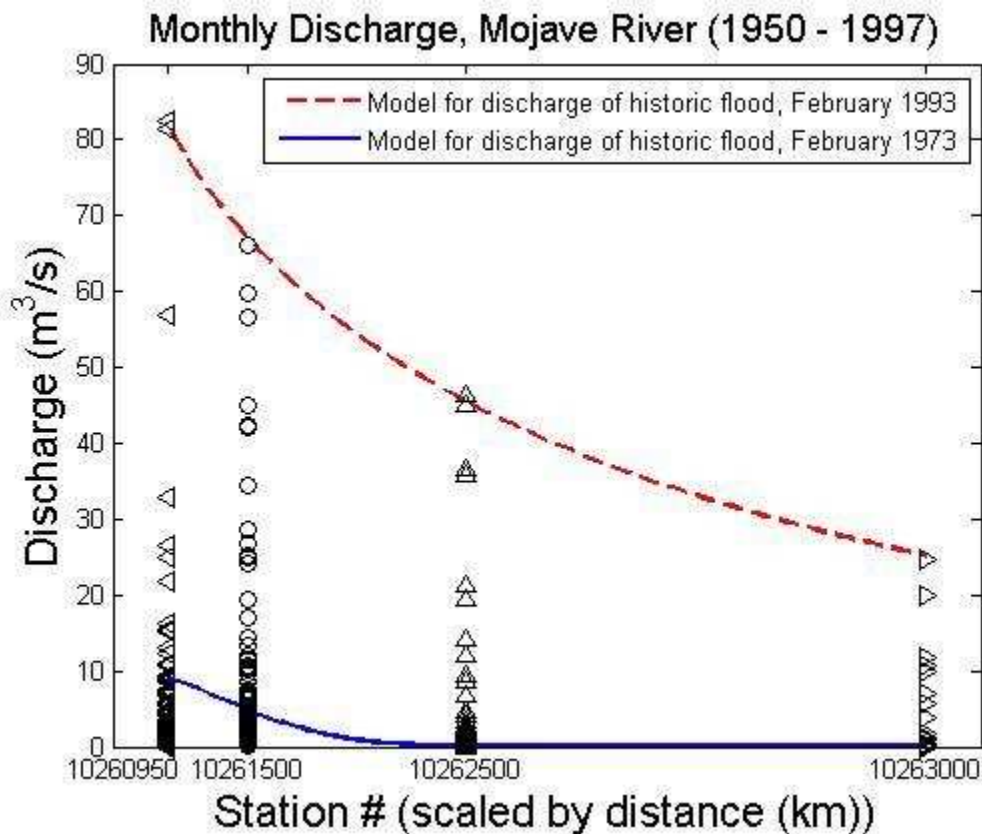
372 Weglarczyk, S., Strupczewski, W. G., Singh, V.P., 2005. Three-parameter discontinuous distributions for
373 hydrological samples with zero values. *Hydrological Processes*, 19: 2899-2914

374 Zular, A., Sawakuchi, A.O., Guedes, C.C.F., Mendes, V.R. Nascimento Jr., D.R., Giannini, P.C.F., 2013.
375 Changes in provenance recorded by OSL sensitivity of quartz, heavy minerals and grain-size data: A SE
376 Brazil coastal barrier case. *Marine Geology*, 335. 64 – 77.



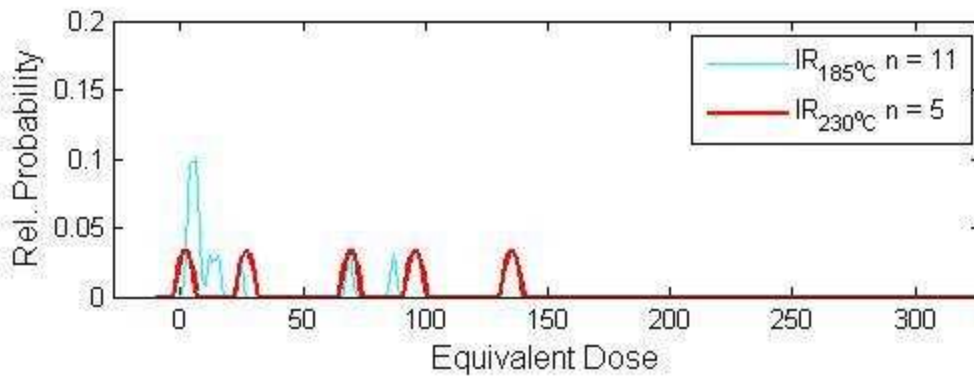
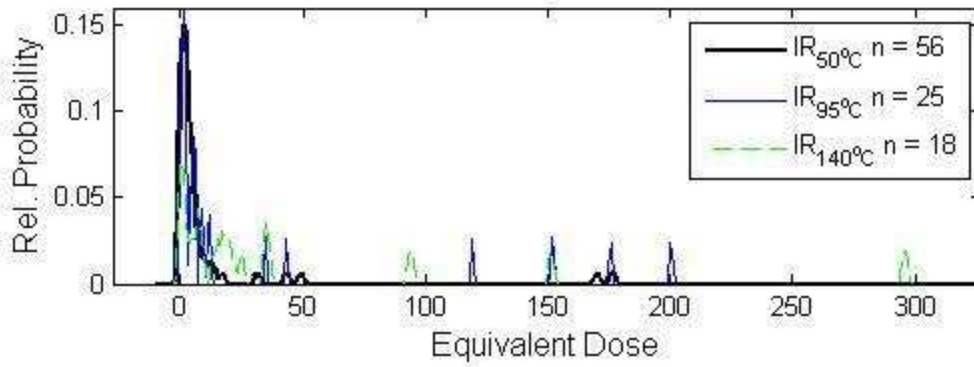


378



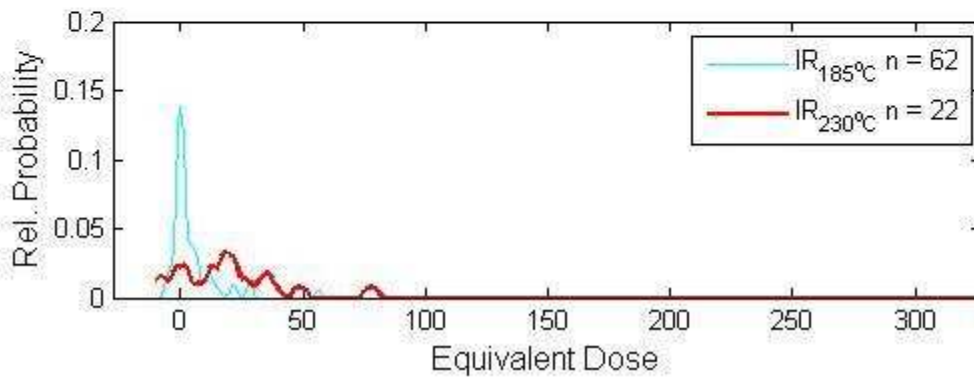
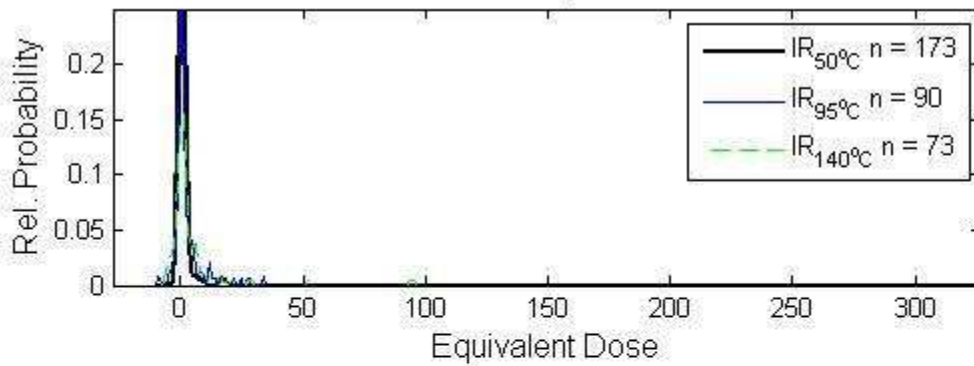
379

Forks MET-pIRIR KDE



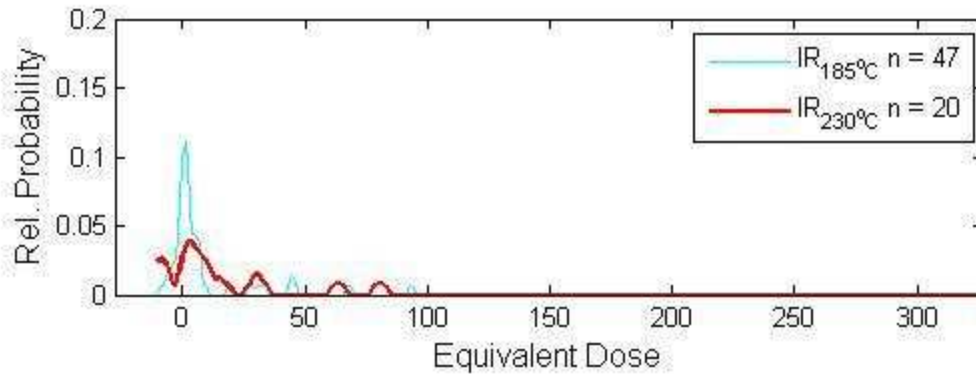
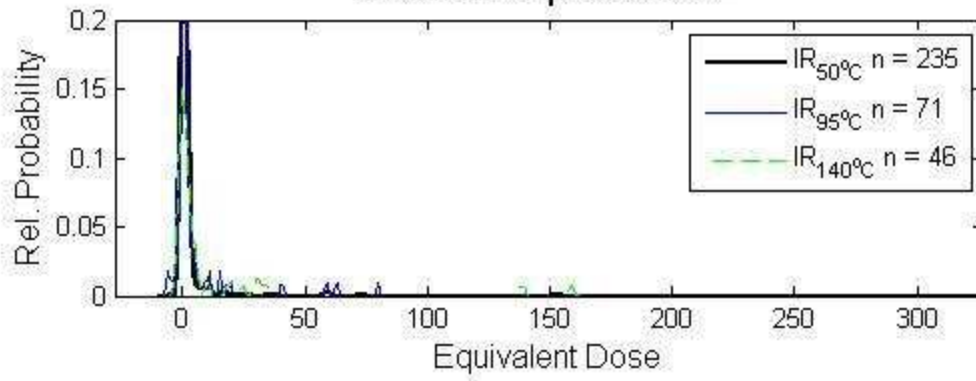
380

Barstow MET-pIRIR KDE



381

Afton MET-pIRIR KDE

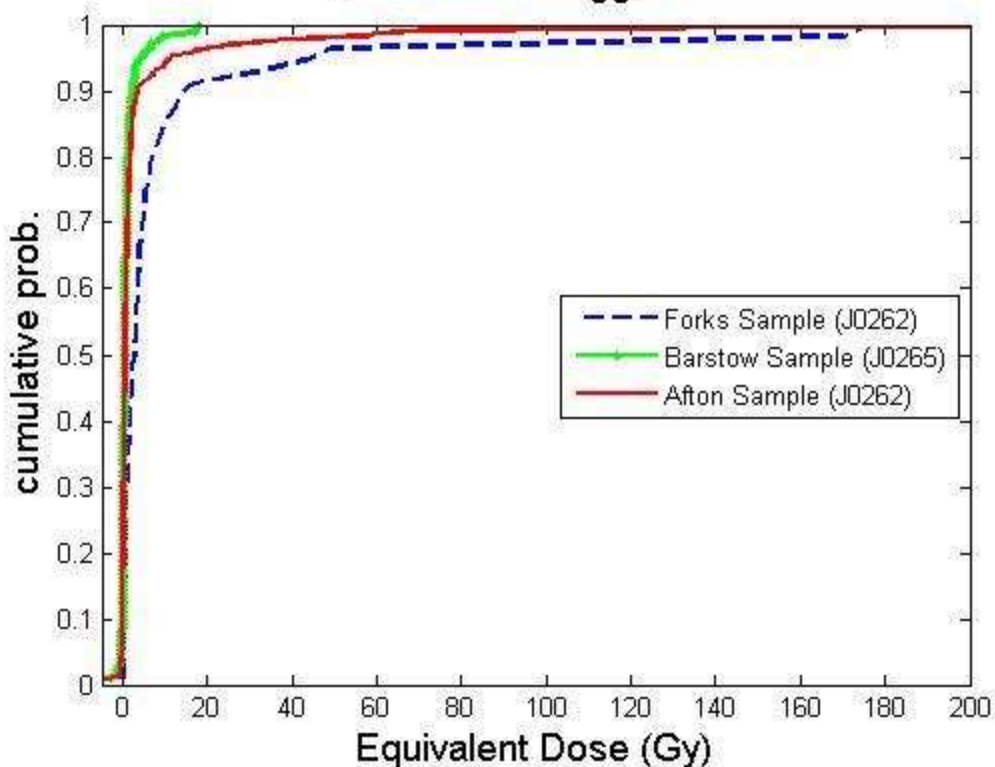


382

383

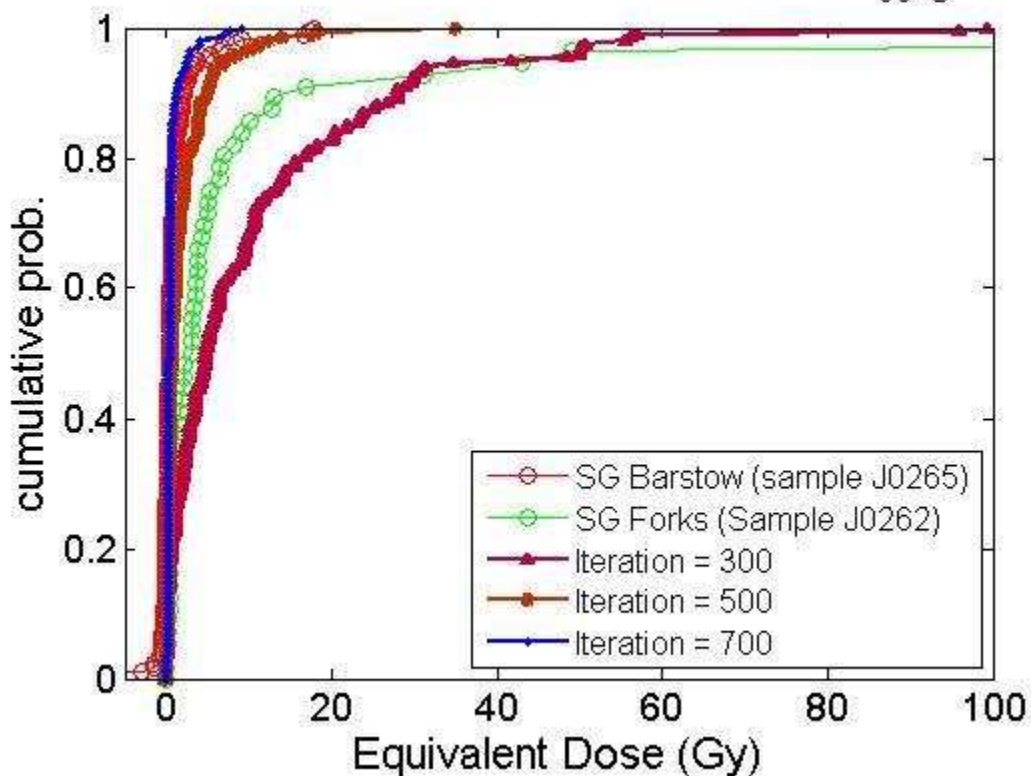
384

Single Grain IR₅₀ Results



385

Single-grain Simulation Results for IR_{50°C}



386